

# Lubricity of Surface Hydrogel Layers

Alison C. Dunn · Juan Manuel Urueña ·  
Yuchen Huo · Scott S. Perry · Thomas E. Angelini ·  
W. Gregory Sawyer

Received: 21 August 2012 / Accepted: 19 November 2012 / Published online: 2 December 2012  
© Springer Science+Business Media New York 2012

**Abstract** Many biological interfaces provide low friction aqueous lubrication through the generation and maintenance of a high water content polymeric surface gel. The lubricity of such gels is often attributed to their high water content, high water permeability, low elastic modulus, and their ability to promote a water film at the sliding interface. Such biological systems are frequently characterized as “soft,” where the elastic moduli are on the order of megapascals or even kilopascals. In an effort to explore the efficacy of such systems to provide lubricity, a thin and soft hydrogel surface layer ( $\sim 5 \mu\text{m}$  in thickness) with a water content of over  $>80\%$  was constructed on a silicone hydrogel contact lens, which has a water content of approximately  $33\%$ . Nanoindentation measurements with colloidal probes on atomic force microscopy (AFM) cantilevers revealed an exceedingly soft elastic modulus of  $\sim 25 \text{ kPa}$ . Microtribological experiments at low contact pressures ( $6\text{--}30 \text{ kPa}$ ) and at slow sliding speeds ( $5\text{--}200 \mu\text{m/s}$ ) gave average friction coefficients below  $\mu = 0.02$ . However, at higher contact pressures, the gel collapsed and friction loops showed a pronounced stick–slip behavior with breakloose or static friction coefficient above  $\mu = 0.5$ . Thus, the ability of the soft surface hydrogel layers to provide lubricity is dependent on their ability to support the applied pressure without dehydrating. These transitions were found to be reversible and

experiments with different radii probes revealed that the transition pressures to be on the order of  $10\text{--}20 \text{ kPa}$ .

**Keywords** Contact lenses · Hydrogels · Microtribology · Lubricity · Stick–slip · Surface modulus

## 1 Introduction and Background

Aqueous lubrication is ubiquitous in nature, and in the eye lubrication relies on the maintenance of a healthy tear film, glycocalyx, and mucin gel layers on the surfaces of the cornea and eyelid epithelia [1]. Mucins and mucinous glycoproteins aggregate to form viscous gels which anchor the aqueous tear film, reduce contact pressures, promote viscous lubrication, and protect the epithelia from shear forces [2, 3]. During the wearing of contact lenses, this delicate balance can be disrupted leading to discomfort and even injury. Soft contact lenses are made from hydrogels that can vary in water content from  $24$  to  $79\%$ , and the lubricity of these lenses after insertion in the eye and during use is directly related to comfort. Contact lenses aim to comfortably correct a patient’s vision over the course of  $\sim 14,000$  blink cycles per day. The study and measurement of the forces incurred during blinks and quantifying lubricity under physiologically relevant contact pressures is motivated by the need to increase comfort over extended time periods.

Hydrogel materials used in contact lenses are designed to be low modulus ( $E' \sim 1 \text{ MPa}$  or below), oxygen permeable (often silicone-based [4]), and thin ( $\sim 100 \mu\text{m}$  in thickness). In this study, a delefilcon A contact lens with a  $\sim 5\text{-}\mu\text{m}$  thick covalently crosslinked soft surface gel layer was used [5, 6]. Following a bio-inspired design, the surfaces of these hydrogels are graded and, as compared to the

A. C. Dunn · J. M. Urueña · T. E. Angelini · W. G. Sawyer (✉)  
Department of Mechanical and Aerospace Engineering,  
University of Florida, Gainesville, FL 32611, USA  
e-mail: wgsawyer@ufl.edu

Y. Huo · S. S. Perry · W. G. Sawyer  
Department of Materials Science and Engineering, University  
of Florida, Gainesville, FL 32611, USA

core material, possess both higher water content and lower modulus. In this design, the core material is a traditional silicone hydrogel that has a water content of 33 %, and through the construction of the interpenetrating anchoring zone the resulting structure produces a gradient of properties and water content. The specific aim is to promote a higher water content (>80 %) at the surface and thereby enhance lubricity by mimicking nature's gel surfaces.

Contact lenses are challenging devices upon which to make fundamental measurements under physiological pressures. They are nearly spherical with a radius of curvature of  $\sim 8$  mm, and most experimental measurements are performed on the apex of the lens surface. At rest, the eyelid pressure is estimated to be  $\sim 1$  kPa [7], which rises to  $\sim 3$ – $8$  kPa during the muscle contractions of a blink. During a blink, the maximum slip velocity is on the order of 100 mm/s and the lubrication regime is hydrodynamic and low friction. Although there are an estimated 14,000 blinks per day, they represent a very small fraction of the contacting conditions that occur during the course of contact lens wear. Ocular motion and the initiation of blinking have sliding speeds below 10 mm/s and are not under hydrodynamic lubrication. It is hypothesized that these ocular moves occur under boundary lubrication, and the lubricity in this regime is the determining factor for lubricity-related comfort. Taken together, tribological measurements of lubricity in contact lenses focuses on low pressure, low speed, and geometries that promote boundary lubrication [8–11]. Glass probes of varying radii of curvature (including flat plates) have been used as counterface materials [8–14]; unfortunately, under conditions of a migrating contact area [15] and curved contact geometries, loads well below 1 mN are required to achieve contact pressures in the low kilopascal range. This combination of macroscopic contact areas, low sliding speeds, sub-mN loads, curved geometries, and measurement in aqueous solutions requires specialized microtribological instrumentation in order to make accurate low friction coefficient measurements [16].

Very low friction coefficients of hydrogels and polymer brushes have been reported under conditions where water films are present within the contact, but such systems have been found to be sensitive to sliding speeds, applied pressure, solvation, and water content [8–11]. Pressure-driven dehydration of hydrogels and polymer brushes can occur under conditions where the water is squeezed from the contact faster than the material can re-establish equilibrium [17, 18], an effect that is pronounced under stationary contact area measurements [15]. Previous work involving PLL-*g*-PEG chains electrostatically adsorbed onto oxide substrates has shown that the architecture or conformation of the polymer chains at the surface highly influences the friction response of the thin film at the sliding contact with

an oxide microsphere [17]. Specifically, low interfacial shear strength was observed when PEG polymer chains assumed an extended brush-like structure under good solvent conditions, highlighting the contribution of interfacial water molecules to lubricity.

We hypothesize high water content surface gel layers, which are thin relative to the characteristic contact dimensions, can promote lubricity in aqueous environments under physiological conditions if they maintain their high water content and develop a low shear interface under direct contact. In this study, the elastic modulus and deformation behavior of these soft surface hydrogel layers was assessed using colloidal probes on atomic force microscopy (AFM) cantilevers, and lubricity was measured using a microtribometer with a moving contact area spherical glass probe [11].

## 2 Materials and Methods

### 2.1 Hydrogels

The Delefilcon A lens has an average thickness of about 100  $\mu\text{m}$ , and is made from a core silicone hydrogel material with an equilibrium bulk water content of 33 % that transitions through an interpenetrating zone to give an  $\sim 5$   $\mu\text{m}$  thick highly hydrated copolymer surface gel layer with >80 % water content (Fig. 1) [5, 19]. This soft surface gel layer does not contain any silicone. For these experiments, the lenses were conditioned by soaking and light agitation for  $\sim 30$  min in borate-buffered saline (Unisol<sup>®</sup> 4, Alcon, Fort Worth, TX). For indentation experiments, the lenses were further conditioned by storage in 10 mL of fresh borate-buffered saline for >24 h in order to remove the effects of packaging solutions. All experiments were performed submerged in borate-buffered saline at room temperature.

### 2.2 Indentation

Nanoscope indentation was performed using AFM (Asylum Research, Santa Barbara, CA), and a 5- $\mu\text{m}$  diameter silica microsphere was employed as the probe, which was affixed on a standard silicon cantilever with a calibrated normal force constant of 5.2 N/m [20]. Modulus values were obtained from indentations performed in a 3-mm diameter region in the center of the front curve surface, and the approach speed of the piezo-driven probe was set at 1  $\mu\text{m/s}$ . The probe was plasma-cleaned before each experiment. The normal force acting on the cantilever was measured as a function of probe displacement. Depth of probe indentation was subsequently calculated as the difference between programmed vertical stage displacement

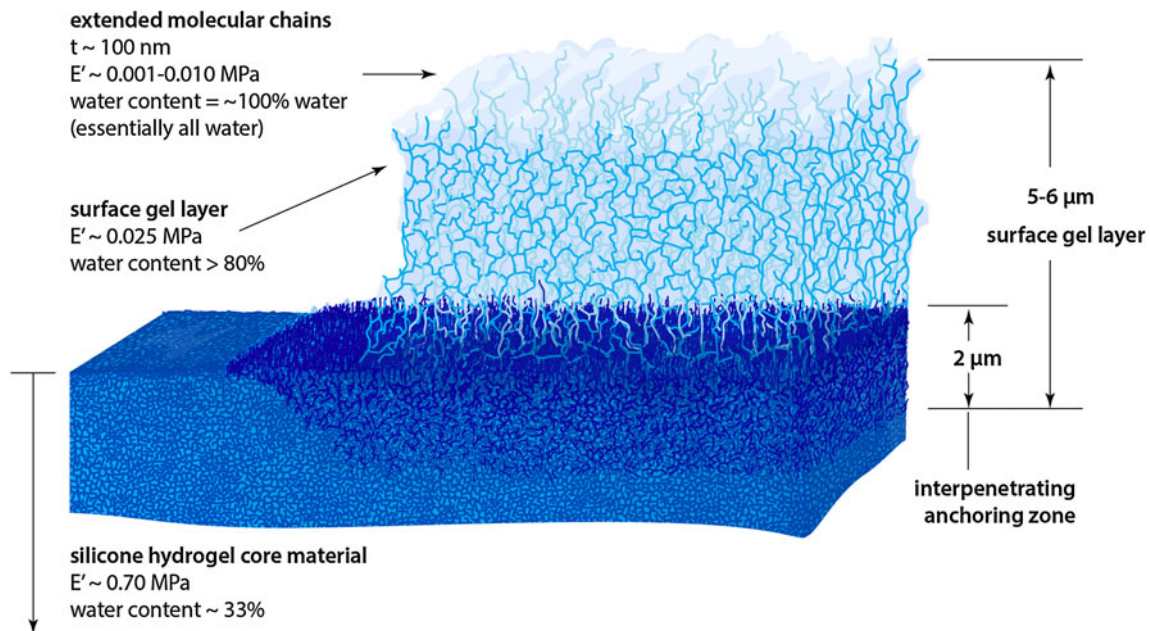


**Fig. 1** A schematic representation of the delectron A lens material including the surface gel layer that is integrated into and onto a silicone hydrogel core material. The entire graded gel layer is estimated to be on the order of  $6\ \mu\text{m}$  in thickness based on AFM

mapping and fluorescence microscopy [5]. The water content of the surface gel layer is greater than 80 %, while the core material is only 33 %

and cantilever deflection. Contact was defined by the point at which the probe appeared to engage with the surface, indicated by a decrease in signal noise and deviation from the zero point normal force.

### 2.3 Friction

Microtribological experiments were performed using a microtribometer (NTR II, CSM Instruments, Peseux, Switzerland) similar to that described in previous work [11]. The contact lens sample was affixed by a clamp to the reciprocating stage in order to ensure relative sliding between the lens surface and a borosilicate glass probe. The clamp was designed to maintain the designed curvature of the lens, and therefore was comprised of a hemispherical base and conformal top with the central area removed for access [21]. A dual titanium flexure with normal and tangential force constants of 75.3 and 111.0 N/m, respectively, was used to both apply and measure a normal load through capacitive displacement sensors. A 1.59-mm radius borosilicate glass probe was adhered to the dual flexure. The contact lens was reciprocated over a  $700\ \mu\text{m}$  long track at  $200\ \mu\text{m/s}$ . Normal forces were controlled to discrete values between  $\sim 100$  to over  $2,000\ \mu\text{N}$ , with at least 20 cycles at each load. To highlight pressure effects, these measurements were repeated on a stiffer cantilever using probe radii of 3.1 and 7.8 mm.

## 3 Results

### 3.1 AFM Colloidal Probe Indentation

Force versus displacement curves were obtained from multiple indentations on the soft surface hydrogel layer in an aqueous bath of phosphate-buffered saline (PBS). Figure 2 depicts a representative dataset in detail, plotting applied normal force versus indentation depth. For indentation depths with the first 200 nm of the surface, an exceedingly low modulus of  $0.025 \pm 0.007\ \text{MPa}$  was fit based on Hertzian contact theory [22]. As the probe penetrated into the surface beyond this depth, the response deviated from the Hertzian contact mechanics relationship.

### 3.2 Friction

The influence of contact pressure on the friction of soft hydrogel surface gel layers has been investigated through a systematic set of friction measurements performed to span from physiological pressures to those reported in other experimental studies. Here, friction coefficients are reported as the average values computed from the friction loops in Fig. 3a using Eq. 1. Each data point indicates the average normal and friction forces from the middle 20 % of the sliding track for one reciprocation cycle at the steady-state normal force.

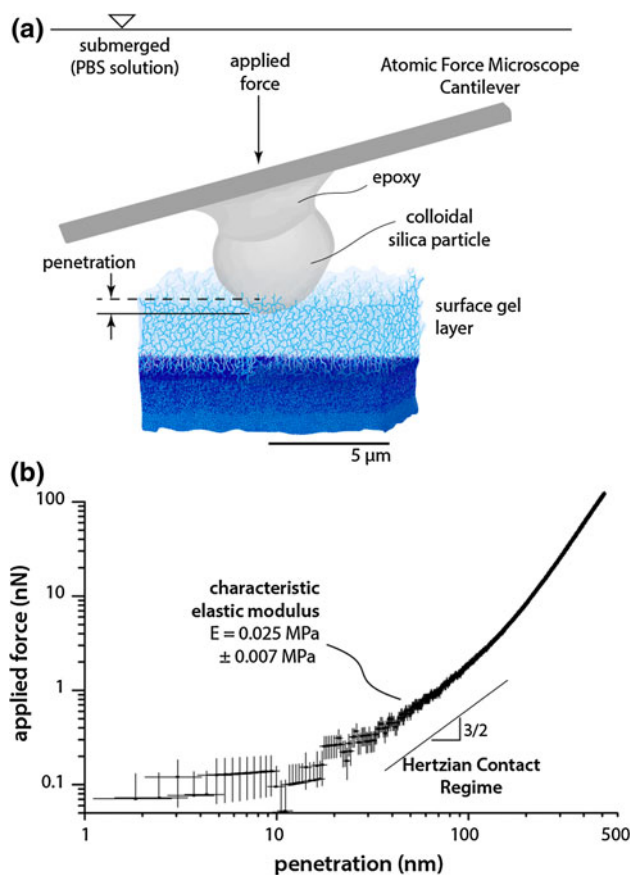


**Fig. 2** **a** A schematic illustration of the colloidal probe indentation experiments performed in an effort to measure the surface gel mechanics. **b** The externally applied force is plotted versus the indentation depth for a 5- $\mu\text{m}$  diameter colloidal silica probe that is mounted onto an AFM cantilever, only the loading portion is shown. The indentation rate was measured to be  $\sim 1 \mu\text{m/s}$ . Associated uncertainty intervals in force and penetration are shown. For shallow indentation depth, Hertzian contact mechanics applies over a range from approximately 40 to 200 nm of penetration; the average elastic modulus computed from this region gives  $E = 0.025 \pm 0.007 \text{ MPa}$  (based on three repeat experiments)

$$\mu = \frac{F_{t,\text{forward}} - F_{t,\text{reverse}}}{2F_n} \quad (1)$$

Friction loops at loads of 163, 797, and 2,056  $\mu\text{N}$  show that the friction coefficients are on the order of  $\mu = 0.02$  during the central, free sliding portion of the experiment. At the applied load of 2,056  $\mu\text{N}$ , significant stick-slip behavior can be clearly identified during motions initiated at the reversal locations (a location where for a short period of time both the probe and the sample are stationary). During stick-slip events, the probe moves with the surface until enough cantilever strain and the resulting reaction forces overcome the interfacial shear force between the surface and the probe. At that point, the probe will vibrate (due to the very low friction coefficient) until it again becomes stuck on the surface, and the entire cycle repeats.

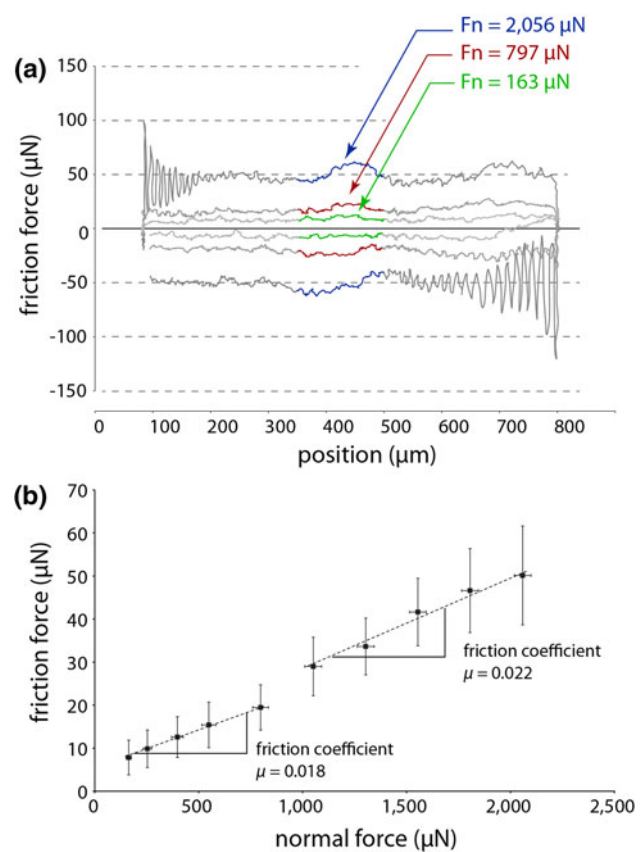


**Fig. 3** **a** Friction loops at loads of 163, 797, and 2056  $\mu\text{N}$  show that the friction coefficients are on the order of  $\mu = 0.02$  during the central, free sliding portion of the experiment. Above contact loads of  $\sim 1,000 \mu\text{N}$ , significant stick-slip behavior can be clearly identified during motions initiated at the reversal locations. **b** A plot of the average friction force and normal force along with the associated experimental uncertainties [16]. The slopes, which give characteristic friction coefficients for the low- and high-pressure regimes, are not particularly different for within the central 20 % of the friction loops as indicated in (a) but are separated based on the observation of persistent stick-slip motions in the reversals

To determine the critical transition pressure for the onset of stick-slip motion, the normal force was systematically increased from 250 to 1,500  $\mu\text{N}$  until the friction force response following reversal points changed from smooth sliding to a stick-slip regime. The onset of stick-slip friction for the 1.59-mm radius probe was at a critical load of  $\sim 1,000 \mu\text{N}$ . Figure 3b shows the friction force response at each normal load. Friction coefficients are shown as the slope of the line on the plot. For this probe, the friction coefficient and associated uncertainties changed from  $\mu = 0.018 \pm 0.006$  below a normal force of 1,000  $\mu\text{N}$  to  $\mu = 0.022 \pm 0.007$  above that load. The average pressure at a normal load of 1,000  $\mu\text{N}$  was approximately 19.1 kPa as calculated from the resulting indentation depth into the sample. This change in friction response, along with the appearance of stick-slip behavior, indicates that there are



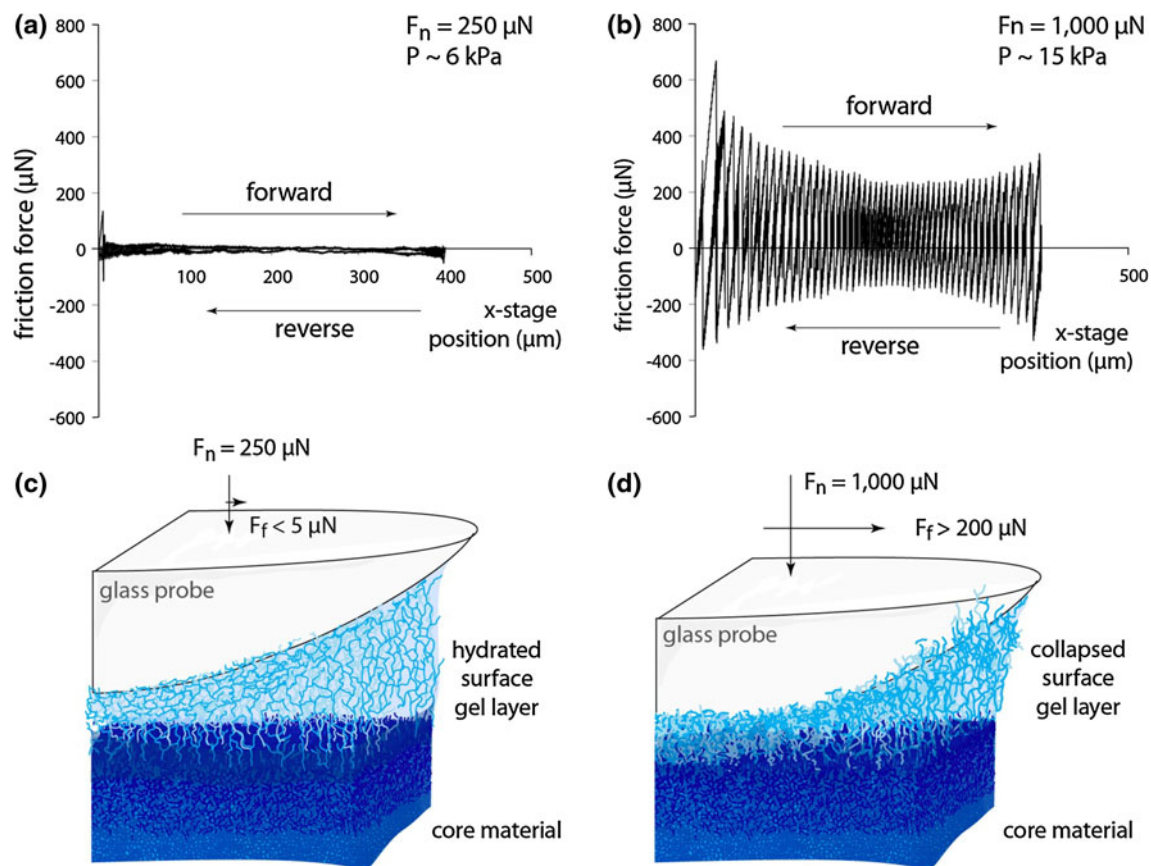


**Fig. 4** Experiments using a very low force cantilever can extend the stick–slip behavior throughout the friction experiment under specific sliding speeds and pin geometries. Here, all experiments are performed with a cantilever of  $82.65 \mu\text{N}/\mu\text{m}$  stiffness in the friction direction and  $138.6 \mu\text{N}/\mu\text{m}$  in the normal load direction. **a** A friction loop at an applied load of  $250 \mu\text{N}$  shows smooth and very low friction forces. **b** A friction loop at an applied load of  $1,000 \mu\text{N}$  reveals significant stick–slip behavior with breakloose friction coefficients on the order of

$\mu = 0.6$ . **c, d** The hypothesis for this transition in friction behavior is that the surface gel layer can collapse under high pressure, and that a collapsed gel layer does not provide low friction aqueous lubrication; however, after breakloose friction is exceeded the rapid slip event exceeds the dehydration rate of the surface gel layer, and the probe can slide freely until it comes to rest, collapses the gel layer, and the process repeats

two very different friction mechanisms in those pressure ranges.

#### 4 Discussion

The design of the defilefilcon A, which has a soft, surface hydrogel layer on a core silicone hydrogel material with a very different water content, is unique among soft contact lenses. The surface modulus fit with the Hertzian model was exceedingly low at  $E' = 25 \pm 7 \text{ kPa}$ ; for comparison, the elastic modulus of single smooth muscle cells and corneal epithelial cells measured with AFM techniques was estimated to be on the order of  $10\text{--}17 \text{ kPa}$  [23, 24].

The friction coefficient of the surface gel layer under low loads was found to be robust and low at  $\mu = 0.018$  (Fig. 3b). The uncertainty intervals plotted in Fig. 3b are actually the uncertainties in measured forces rather than the

fluctuations in friction coefficient, which in the case of the lowest loads were significantly lower. Overall, the average friction coefficient and associated uncertainties were estimated to be  $\mu = 0.020 \pm 0.006$  for experiments performed at  $10\text{--}30 \text{ kPa}$ .

The mechanism underlying the stick–slip behavior is hypothesized to be the result of local contact pressures collapsing the soft surface hydrogel layer and forcing water squeeze-out (Fig. 4c, d). In order to explore this transition threshold, a series of experiments were performed with slightly stiffer cantilever at a slower sliding speed of  $2 \mu\text{m}/\text{s}$  and larger probe radius of  $3.1 \text{ mm}$  (Fig. 4a, b). A clear, repeated saw-tooth pattern in high friction of  $\mu \sim 0.5$  emerged under an applied load of  $1,000 \mu\text{N}$  (Fig. 4b). This stick–slip friction occurs when the force from the cantilever lateral deflection exceeds the static friction coefficient in the contact, which is a function of the sample/probe elastic mismatch and the measurement conditions. The probe

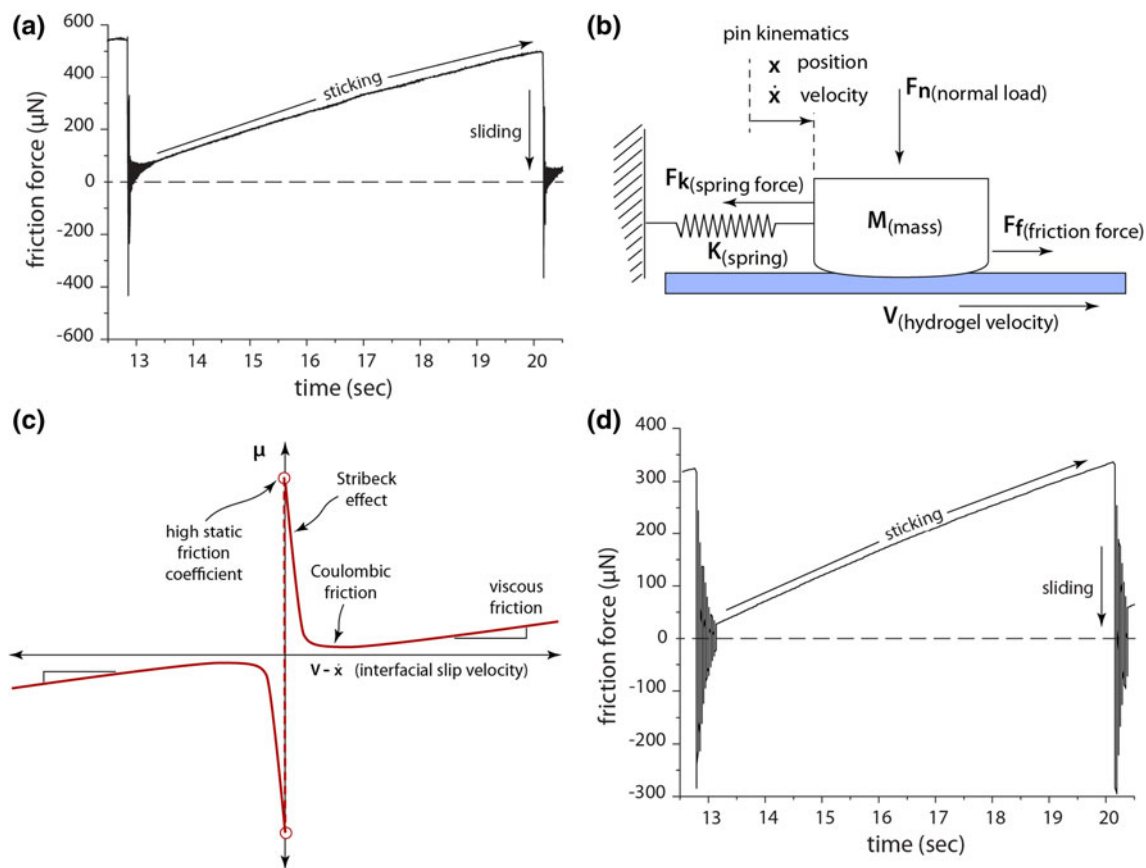


**Fig. 5** **a** Low speed, high load conditions emphasize the stick–slip behavior as shown here in the friction force response over time. The breakloose friction force is  $\sim 500 \mu\text{N}$  and drops to less than  $100 \mu\text{N}$  after the slip event. Applied normal load was  $1,000 \mu\text{N}$ . The probe exhibits high-frequency ringing across the surface after each instance of sticking. **b** The oscillation can be modeled as a spring and mass system damped by the friction force between the surface gel layer and

the probe. **c** The transitions between stick–slip and smooth sliding give rise to a velocity-dependent friction model. The interfacial slip velocity is the difference between the prescribed sliding speed and the velocity of the probe. At low slip velocities, the static friction coefficient is high. At high slip velocities, viscous friction dominates. **d** This dynamic response is captured by numerical simulation including the velocity-dependent friction model shown in (c)

then rapidly slips across the nascent soft surface hydrogel region and “rings” at a resonant mode prior to again becoming stuck. This stick–slip pattern in friction was not detectable at forces below  $500 \mu\text{N}$  ( $P \sim 10 \text{ kPa}$ ), and the friction coefficient remained below  $\mu = 0.021$  in the middle 20 % of the track. We hypothesize that this increase in friction coefficient of over tenfold with associated stick–slip character is due to the collapsing of the soft surface hydrogel layer, which leads to a high polymer concentration at the surface and high static friction. The relatively low stress  $< 20 \text{ kPa}$  at which this transition occurs is on the order of stresses produced in polymer brush thin films as micro-actuators [25–27], and is on the same order of magnitude as the elastic modulus measured from the colloidal probe experiments. Increases in friction coefficient of this magnitude have been previously documented with the collapse of PLL-*g*-PEG brush systems, where brush collapse has been initiated by varying the solvent quality [28, 29].

The dynamic oscillatory response of the probe that occurs after a slip event can be modeled as spring mass system (Fig. 5b) with a non-linear continuously differentiable friction model (Fig. 5c), following the work of Makkar et al. [30]. The transitions between stick–slip and smooth sliding give rise to a slip velocity-dependent friction model (Fig. 5c). The interfacial slip velocity is the difference between the prescribed sliding speed and the velocity of the probe. At low slip velocities, the static friction coefficient is high. At high slip velocities, the low friction of the nascent surface is maintained because the permeability of the surface hydrogel layer prevents instantaneous collapsing of the gel. A numerical simulation of this microtribological system captures the basic phenomena (Fig. 5d), where the mass is  $1 \text{ g}$ , the applied load is  $1 \text{ mN}$ , the combined lateral spring constant is  $27 \text{ mN/mm}$ , and the plate velocity is  $2 \mu\text{m/s}$ .

Based on simulations of the contact pressure distribution and lubricity measurements under multiple loads, speeds,

and probe radii, the threshold transition for these surface hydrogel layers from smooth sliding to a stick–slip behavior is on the order of 10–20 kPa, which is in the same order as the measured elastic modulus of the surface gel layer and further supports the assertion that the stick–slip phenomena is related to the collapse of the surface gel layer. For applications in the eye, the lubricity of such a surface hydrogel layer will be preserved as the ocular applied pressures are on the order of 1–8 kPa.

## 5 Concluding Remarks

- (1) A low modulus and high water content soft surface hydrogel layer was shown to provide consistent low friction sliding under boundary lubrication in an aqueous environment.
- (2) Stick–slip behavior was observed at pressures above 10–20 kPa and is assumed to be the result of a pressure-induced collapse and dehydration of the soft surface hydrogel layer. In addition, the importance of performing tribological evaluation of contact lenses at low contact pressures is revealed.
- (3) Measurements of the soft surface hydrogel layer show a characteristic elastic modulus of 25 kPa, which is similar to estimated contact pressures at transition.

**Acknowledgments** The authors gratefully acknowledge Drs. Pruitt and Sentell of Alcon Laboratories for many useful discussions on contact lenses and hydrogels, and for providing the delefilcon A lenses. This work was funded by Alcon Laboratories.

## References

1. Davidson, H.J., Kuonen, V.J.: The tear film and ocular mucins. *Vet. Ophthalmol.* **7**(2), 71–77 (2004)
2. Coles, J.M., Chang, D.P., Zauscher, S.: Molecular mechanisms of aqueous boundary lubrication by mucinous glycoproteins. *Curr. Opin. Colloid Interface Sci.* **15**(6), 406–416 (2010). doi:10.1016/j.cocis.2010.07.002
3. Yakubov, G.E., Mccoll, J., Bongaerts, J.H.H., Ramsden, J.J.: Viscous boundary lubrication of hydrophobic surfaces by mucin. *Langmuir* **25**(4), 2313–2321 (2009). doi:10.1021/La8018666
4. Wang, J.J., Li, X.S.: Preparation and characterization of interpenetrating polymer network silicone hydrogels with high oxygen permeability. *J. Appl. Polym. Sci.* **116**(5), 2749–2757 (2010). doi:10.1002/App.31902
5. Qiu, Y., Pruitt, J.D., Thekveli, S.J., Tucker, R.C., Nelson, J.: Silicone hydrogel lenses with water-rich surfaces. USA Patent 20120026458
6. Qiu, Y., Samuel, N.T., Pruitt, J.D., Kolluru, C., Medina, A.N., Winterton, L.C., Wu, D., Qian, X., Nelson, J.: Silicone hydrogels with a crosslinked hydrophilic coating. USA. Patent 20120026457
7. Shaw, A.J., Collins, M.J., Davis, B.A., Carney, L.G.: Eyelid pressure and contact with the ocular surface. *Invest. Ophthalmol. Vis. Sci.* **51**(4), 1911–1917 (2010). doi:10.1167/Iovs.09-4090
8. Roba, M., Duncan, E.G., Hill, G.A., Spencer, N.D., Tosatti, S.G.P.: Friction measurements on contact lenses in their operating environment. *Tribol. Lett.* **44**(3), 387–397 (2011). doi:10.1007/s11249-011-9856-9
9. Zhou, B., Li, Y.T., Randall, N.X., Li, L.: A study of the frictional properties of senofilcon—a contact lenses. *J. Mech. Behav. Biomed.* **4**(7), 1336–1342 (2011). doi:10.1016/j.jmbbm.2011.05.002
10. Nairn, J.A.: Measurement of the friction and lubricity properties of contact lenses. In: ANTEC: The Plastics Challenger: A Revolution in Education 1995, p. 3384. Society of Plastics Engineers
11. Rennie, A.C., Dickrell, P.L., Sawyer, W.G.: Friction coefficient of soft contact lenses: measurements and modeling. *Tribol. Lett.* **18**(4), 499–504 (2005). doi:10.1007/s11249-005-3610-0
12. Ngai, V., Medley, J.B., Jones, L., Forrest, J., Teichroeb, J.: Friction of contact lenses: Silicone hydrogel versus conventional hydrogel. In: 31st Leeds-Lyon Symposium on Tribology, Trinity and All Saints College, Horsforth, Leeds, 2004. Tribology and Interface Engineering Series, pp. 371–379 (2005)
13. Tighe, B.: Measurement of frictional characteristics of contact lenses. In: BCLA Annual Clinical Conference, Birmingham, 2006, pp. 201–202. *Contact Lens & Anterior Eye* (2006)
14. Tucker, R.C., Quinter, B., Patel, D., Pruitt, J.D., Nelson, J.: Qualitative and Quantitative Lubricity of Experimental Contact Lenses. Paper presented at the ARVO, Fort Lauderdale, FL, 10 May 2012
15. Bonnevie, E.D., Baro, V.J., Wang, L., Burris, D.L.: Fluid load support during localized indentation of cartilage with a spherical probe. *J. Biomech.* **45**(6), 1036–1041 (2012). doi:10.1016/j.jbiomech.2011.12.019
16. Schmitz, T.L., Action, J.E., Ziegert, J.C., Sawyer, W.G.: The difficulty of measuring low friction: uncertainty analysis for friction coefficient measurements. *J. Tribol-T Asme* **127**(3), 673–678 (2005). doi:10.1115/1.1843853
17. Perry, S.S., Yan, X.P., Limpoco, F.T., Lee, S., Muller, M., Spencer, N.D.: Tribological properties of poly(L-lysine)-graft-poly(ethylene glycol) films: influence of polymer architecture and adsorbed conformation. *ACS Appl Mater Inter* **1**(6), 1224–1230 (2009). doi:10.1021/Am900101m
18. Dunlop, I.E., Thomas, R.K., Titmus, S., Osborne, V., Edmondson, S., Huck, W.T.S., Klein, J.: Structure and collapse of a surface-grown strong polyelectrolyte brush on sapphire. *Langmuir* **28**(6), 3187–3193 (2012). doi:10.1021/La204655h
19. Thekveli, S.J.: Structure–property relationship of delefilcon A lenses. Paper presented at the BCLA Conference 2012, Birmingham, UK
20. Hutter, J.L., Bechhoefer, J.: Calibration of atomic-force microscope tips. *Rev. Sci. Instrum.* **64**(7), 1868–1873 (1993)
21. Uruena, J.M., Dunn, A.C., Sawyer, W.G.: Contact lens boundary lubrication and friction reduction with hyaluronic acid. *Tribol. Lubr. Technol.* **67**(12), 14–15 (2011)
22. Johnson, K.L.: *Contact Mechanics*. Cambridge University Press, Cambridge (1987)
23. Kuznetsova, T.G., Starodubtseva, M.N., Yegorenkov, N.I., Chizhik, S.A., Zhdanov, R.I.: Atomic force microscopy probing of cell elasticity. *Micron* **38**(8), 824–833 (2007). doi:10.1016/j.micron.2007.06.011
24. Straehla, J.P., Limpoco, F.T., Dolgova, N.V., Keselowsky, B.G., Sawyer, W.G., Perry, S.S.: Nanomechanical probes of single corneal epithelial cells: shear stress and elastic modulus. *Tribol. Lett.* **38**(2), 107–113 (2010). doi:10.1007/s11249-010-9579-3
25. Abu-Lail, N.I., Kaholek, M., LaMattina, B., Clark, R.L., Zauscher, S.: Micro-cantilevers with end-grafted stimulus-

- responsive polymer brushes for actuation and sensing. *Sensor Actuat. B* **114**(1), 371–378 (2006). doi:[10.1016/j.snb.2005.06.003](https://doi.org/10.1016/j.snb.2005.06.003)
26. Kim, P., Zarzar, L.D., Zhao, X.H., Sidorenko, A., Aizenberg, J.: Microbristle in gels: toward all-polymer reconfigurable hybrid surfaces. *Soft Matter* **6**(4), 750–755 (2010). doi:[10.1039/B920392c](https://doi.org/10.1039/B920392c)
27. Huck, W.T.S.: Responsive polymers for nanoscale actuation. *Mater. Today* **11**(7–8), 24–32 (2008)
28. Muller, M.T., Yan, X.P., Lee, S.W., Perry, S.S., Spencer, N.D.: Lubrication properties of a brushlike copolymer as a function of the amount of solvent absorbed within the brush. *Macromolecules* **38**(13), 5706–5713 (2005). doi:[10.1021/Ma0501545](https://doi.org/10.1021/Ma0501545)
29. Vyas, M.K., Schneider, K., Nandan, B., Stamm, M.: Switching of friction by binary polymer brushes. *Soft Matter* **4**(5), 1024–1032 (2008). doi:[10.1039/B801110a](https://doi.org/10.1039/B801110a)
30. Makkar, C., Hu, G., Sawyer, W.G., Dixon, W.E.: Lyapunov-based tracking control in the presence of uncertain nonlinear parameterizable friction. *IEEE Trans. Automat. Contr.* **52**(10), 1988–1994 (2007). doi:[10.1109/Tac.2007.904254](https://doi.org/10.1109/Tac.2007.904254)